Svedberg Open
DISSEMINATION OF KNOWLEDGE

International Journal of Artificial Intelligence and Machine Learning

Publisher's Home Page: https://www.svedbergopen.com/

Research Paper Open Access

Automatic lung tumor segmentation and classification based on improved U-Net assisted hybrid deep learning approach

Gottumukkala Thanmaya Tejaswi[1], Nulaka Srinivasu[2], Pardha Saradhi Varma Gottumukkala[3]

[1]Research scholar, Department of Computer Science and Engineering, Koneru Lakshmaiah Education Foundation, Vijayawada, Andhra Pradesh-522302. India, Email: thanmayatejaswi@gmail.com, ORCID: 0009-0004-6811-6867

[2]Professor, Department of Computer Science and Engineering, Koneru Lakshmaiah Education Foundation, Vijayawada, Andhra Pradesh -522302, India, Email: srinivasu28@kluniversity.in, ORCID: 0000-0002-9593-3916

[3] Professor, Department of Computer Science and Engineering, Koneru Lakshmaiah Education Foundation, Vijayawada, Andhra Pradesh -522302. India, Email: gpsvarma@gmail.com, ORCID: 0000-0002-4885-1678

Abstract

Early lung tumor detection is crucial because symptoms often appear late. The cloud revolutionize early diagnosis through real-time data collection and on-device model training. Machine learning and image processing techniques have already shown promise in identifying lung tumor from scans. Traditional methods struggled with less accuracy and less speed seems to be the major limitations. Early detection saves lives by enabling treatment before the cancer seals airways and infections set in. For the early diagnosis of lung tumor, the proposed methodology is developed with novel segmentation, feature extraction and classification models under improved U-Net model, stacked auto encoder and dilated depth-wise separable convolutional network assisted bidirectional long short term memory model (DDWC-Bi-LSTM) respectively. To segment the medical images, U-Net is improved with guided attention mechanism. To further validate the efficiency of proposed approach, the dataset is utilized in terms of accuracy, precision, recall, F1-score, and error. Proposed technique obtain an accuracy of 96.62% and 97.86% for kaggle and Medical Segmentation Decathlon lung datasets respectively.

Keywords: lung tumor, improved U-Net, dilated convolutions, bi-directional LSTM, segmentation, guided attention.

1. Introduction

With the growth of technology, the use of technological development in the healthcare system has gathering huge attention worldwide. The use of artificial intelligence, cloud computing and internet of things (IoT) in healthcare system [1-3] has solved many biomedical issue. Owing to these technology one can remotely their health conditions [4, 5]. The IoT devices could collect health data from various patients and non-patients to cross validate the health condition [6, 7], which are stored in cloud server for future uses. The cloud could offer wide storage space for storing varied data structures. Also to solve the medical detection issue the cloud could offer artificial intelligence models to detect disease. Increasing death rate due to cancer is increasing around the world. According to the analysis of world health organization, a highest death rate has been occurred due to lung cancer [8] and the second one is breast cancer [9]. The lung cancer is mainly caused due to the risk factors of environmental and globalization.

The challenges faced for the early detection of lung cancer includes no symptoms with age factors, breathing problem and years of smoking activity [10]. Researchers identified that survival rate of lung cancer is increased when it is detected at the earliest [11]; however, it is a tedious process. Hence computed aided diagnosis system [12] is widely used for accurate detection process. Initially, the machine learning based models are used to diagnose disease from CT scan images. Some of the well-known machine learning methods used for the diagnosis of lung cancer is given below.

K-nearest neighbor (KNN) algorithm is used for the lung cancer detection in which the features are selected by genetic algorithm [13]. The accuracy of detection relies on quality of inputs without a significant preprocessing an accurate result is not obtained. The support vector machine is used with firefly algorithm [14] to prognosis lung nodules. The classifier uses the segmented output from fuzzy C-clustering process, which lacks its performance when image size in a dataset is varied. Hence a random forest hybridized with boosting algorithm [15] is reported on LIDC data. However, the error rate in the system is increased; thus the DICOM CT images are used with machine learning algorithms [16] for accurate detection of lung tumor. In that dataset, certain algorithms such as Naive Bayes, support vector machine, Decision tree and Logistic Regression etc. [17] are examined. Those algorithms resulted in poor accuracy due to insufficient data for training and also, the response time for the execution is higher. Due to this the researchers are fascinated to use machine learning algorithm with deep learning methods.

The ensemble learning using discrete Adaboost classifier [18] is developed that uses generalized neural network to process distinct features of CT image. The maximum likelihood boosting algorithm with weight optimized network [19] is used with separate feature selection process. The ensemble classifier improves the accuracy by occupying more memory space and also, the models are computationally expensive. Hence the deep learning architectures are adopted with increasing learning characteristics. The advancements in deep learning help researchers to look over the solution to early lung tumor prognosis system [20]. Hence recurrent neural network is used with principal component analysis and t-distributed stochastic neighbor embedding method. The feature extraction method is based on correlation factor, which is brought by using self-adaptive sea lion optimization [21]. The algorithm evaluates the weight for the detection of relevant feature. A hybrid classifier is developed by using multi-layer region proposal neural network [22] which is hybridized with enhanced region based fully connected neural network. The algorithm uses position sensitive score map for the detection of lung tumor. For a high dimensional complex data the subspace clustering provides excellent performance hence a self-supervised deep multilevel subspace clustering approach [23] is used for lung tumor detection in hyperspectral images. Even though there are many methods available for the detection process, the problem associated with training dataset is still in research, the existing deep leaning based methods has high number of evaluation parameters with respect to accuracy and also lack of training data reduce the knowledge about test data. Hence it is necessary to provide compensation for parameter issue, complexity issue and training data issue, which is dealt by this proposal.

1.1 Problem statement & Motivation

Early detection of lung tumors remains challenging due to the absence of symptoms in some patients, the wide range of individuals susceptible across age groups, and the difficulty in pinpointing tumors in smokers with existing breathing problems – all factors that make identifying lung cancer in its early stages critical. Moreover the risk of death is increased due to inconsistent treatment and monitoring. Researchers have tackled the challenges of lung cancer detection using a combination of techniques: segmentation, detection, and classification. But still, there are few limitations of the conventional approaches that are not sufficient in early detection, less efficient in accuracy rate, not suitable for stage classification, etc. To overcome these various models are used in existing studies like KNN, Convolutional Neural Network (CNN), Support Vector Machine (SVM), and Multilayer Perceptron (MLP). The major drawbacks of these models are unable to fit in the current pandemic scenario where the physical medication is impossible. The advancements on Internet of Things, cloud server system, big-data techniques, and sensor units are able to improve the electronic diagnosis, detection of lung cancer on early stage, detection of localization, tumor segmentation, stages classification, regular monitoring, E-treatment, etc. Motivated by these advanced technique performance and adopted them to utilize in the healthcare industry. Advanced and hybrid techniques are introduced based on current scenario challenges is introduced. The main contributions of this work is listed below:

- To pre-processed image by using gaussian amended bilateral filter for produce accurate classification performance.
- To segment pre-processed image by using improved U-net model for identify accurate tumor region

- To tackle feature dimensionality issues in tumor detection, we use a stacked autoencoder model for feature extraction, enabling effective reduction in the dimensionality of the data without significant loss of relevant information.
- To improve classification accuracy and computational efficiency, this research propose a hybrid deep learning model consisting of a Dilated Depthwise Separable Convolutional Network (DDWC) integrated with a Bidirectional Long Short-Term Memory (BiLSTM) network.

The remaining of the paper is structured as follows: Section 2 reviews some of the recent related researches based on lung tumor detection. Section 3 elaborates the proposed methodology of this work. Results and evaluation are discussed in Section 4. Finally, Section 5 provides the conclusion.

2. Related study

Various research studies on lung tumor detection is reviewed in this section.

The modified DenseNet with feature selection algorithm is reported by Lanjewar et al. [24] for the diagnosis of lung cancer. The denseNet201 architecture is modified by incorporating number of layers in the network with reduced parameters. The number of features in DenseNet is high hence to reduce the redundant feature vector the features are treated by extra tree classifier and maximum relevance minimum redundancy feature selection methods. The feature obtained from the neural network was used in varied machine learning algorithms such as support vector machine, logistic regression (LR), k-nearest neighbor, decision tree (DT), random forest (RF) and Gaussian Naïve Bayes (GNB) methods. The number of evaluation metric in the study was high and also the processing times of machine learning algorithms are high.

To improve the early stage identification of lung cancer, IoT technology was utilized by Pawar et al. [25]. To control the death rate and early detection for such disease, the author has suggested extended convolutional neural network embedded with blockchain technology. The IoT devices collect some data such as weight, face features, size of upper chest etc. for the detection purpose. Each of the features is trained individually to the neural network to achieve high detection accuracy. The misclassification rate will be high since, there is not separate knowledge system for processing features.

The automatic detection of lung tumor is achieved by using ensemble classifier was reported by Shakeel et al. [26]. The dataset comprised of non-small cell lung cancer CT scan data obtained from cloud server. The images are preprocessed by using multi-level brightness preserving approach that would reduce noise and preserve the quality of image. Then the region of interest is segmented by using improved deep neural network with multiple layers to finely extract the features of lung tumor was presented. From the segmented portion, the optimized features are selected by using hybrid spiral optimization intelligent generalized rough set approach. Then the features are used to evaluate the stages of lung tumor by using ensemble classifier comprising boosting process. The use of ensemble classifier increases the execution time and expensive.

The cloud based heterogeneous processing of lung tumor image data from internet of medical things was realized by Gu et al. [27]. Since the data was collected from various IoT devices, it might be image or data hence a data integration system is necessary. Then the data was preprocessed and a structured data were framed. The intelligent feature extraction algorithm was used to evaluate the similarity between query image and preprocessed image. Then an artificial intelligence system is used to detect the lung cancer from heterogeneous data. LIDC-IDRI, TCIA and TCGA dataset are utilized for experimentation and to detect the similarity.

For the reduction of death rate due to lung tumor detection, a cloud based system was reported by Kasinathan et al. [28] by integrating segmentation, detection and stage classification modules. Initially, author had performed segmentation by using active contour scheme followed by that multi-layer convolutional neural network (M-CNN) was utilized for classification. This would ensure small and non-small cell lung cancer types. The adopted scheme was examined on LIDC and CT DICOM images, which are preprocessed for noise removal. However, the curvy edges of the tumor were segmented by using snakes' model so that contour line gather the information about both distinct and control point. The accuracy of the model is poor since, the author has used a small dataset thus the misclassification is high.

Faruqui et al. [29] has used both CT scan data and medical IoT data for analysis. The author has utilized LungNet which comprises of hybrid deep convolutional neural network (DCNN) with twenty two cascaded convolutional layers to process CT image and IoT data. The adopted network combines the latent features from both heterogeneous data. Thereby varied stages with different grades of lung tumor disease were detected.

An intelligent health care monitoring system was developed by Mishra et al. [30] for the detection of lung cancer risk factors. The continuous data for processing was obtained through IoT devices that collect data remotely from patients. The data collected from IoT has most irrelevant and unwanted data which was processed by greedy best first search (GBFS) algorithm. The obtained features are directly applied to random forest classifier for detection purpose. Due to the increasing number of decision trees, the algorithm is much slower than other. Table 1 outlines the literature review analysis.

Table 1: Existing study analysis

Author & references	Objective	Methods	Performance metrics	Limitation
Lanjewar et al. [24]	To diagnose the lung cancer using feature selection and ML classifiers	Modified DenseNet-201, SVM, LR, KNN,RF, GNB, DT	Accuracy, dice score, Matthews correlation coefficient (MCC), kappa score	High processing time
Pawar et al. [25]	To predict the lung cancer using extended CNN	VGG-16, U-Net	Accuracy	Efficient feature extraction and segmentation methods are not utilized.
Shakeel et al. [26]	To predict the lung cancer using optimized image processing and ML techniques	Deep neural networks, ensemble classifier	Kulczynski index (KI), accuracy, specificity, precision, folks mallows index(KMI), recall, F-measure, rand index (RI) and Russel– Rao index (RRI)	Not mentioned
Gu et al. [27]	To detect the lung cancer using cloud based deep learning model.	Data integration system	Cosine similarity	Classification performance metrics are failed to analyze.
Kasinathan et al. [28]	To diagnose the lung tumor detection using cloud based deep learning model.	M-CNN	Accuracy, precision, recall	Large database is necessary for accurate detection.
Faruqui et al. [29]	To diagnose the lung cancer using wearable sensor and CT data	DCNN	Accuracy	High computational complexity
Mishra et al. [30]	To develop a lung cancer risk detection strategy using IoT	GBFS, RF classifier	Accuracy, F-score, sensitivity, specificity, latency	Limited amount of data images.

Various shortcomings are received for accurate lung cancer detection from previous literature. High processing time [24], lack of efficient feature extraction approach and segmentation approach [25], limited amount of data [28] [30] and high computational complexity [29] are the major limitations observed from this literature. The proposed method is intended to overcome these kind of drawbacks and to introduce a novel lung tumor detection system based on segmentation and classification.

3. Proposed Methodology

For the early detection of lung tumor detection, the CT image data from cloud server is considered. The data consist of healthy and affected lung images. The threshold based segmentation has the problem of segmenting the background information as region of interest hence a clustering based segmentation approach is suggested in this research.

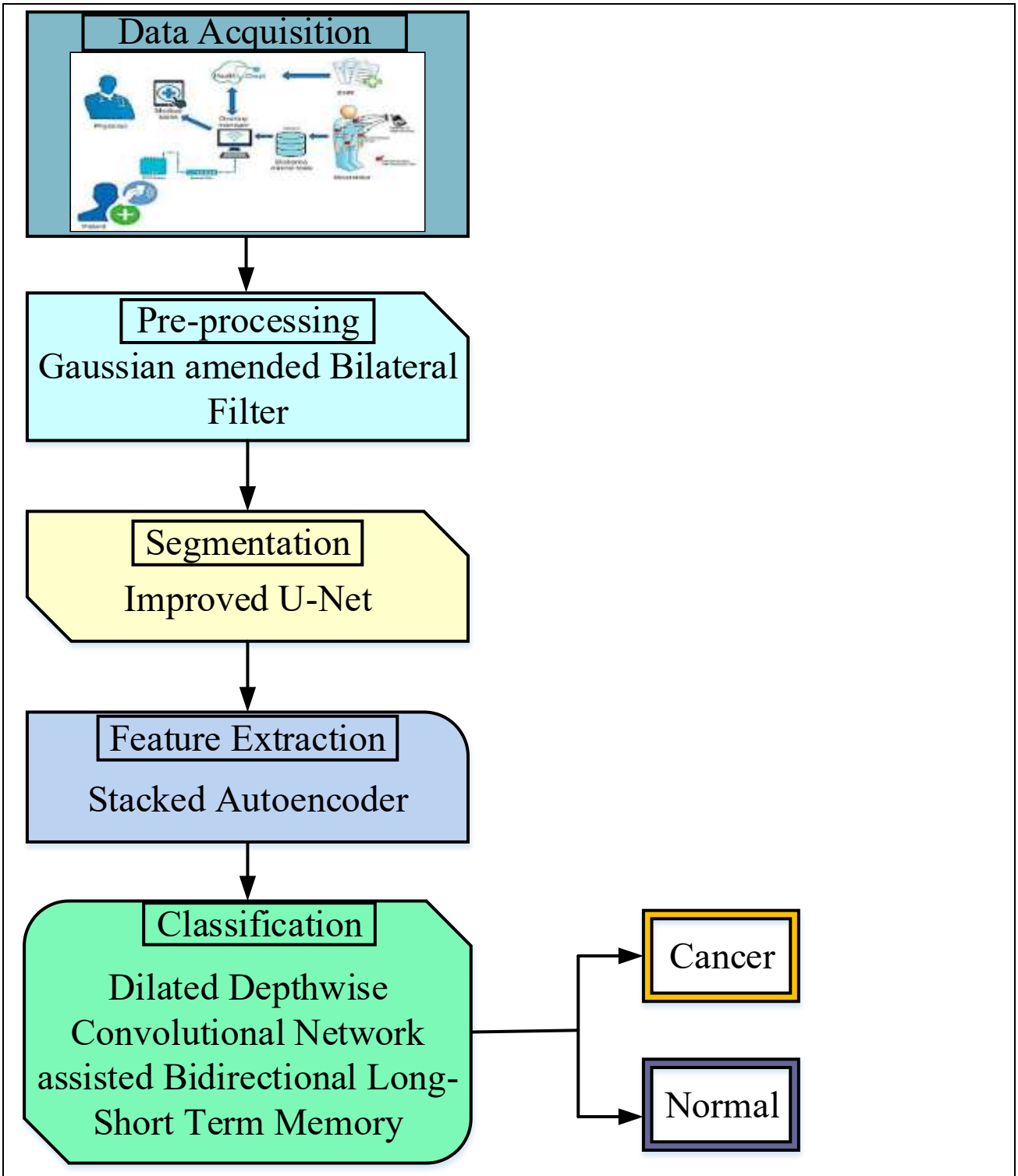

Fig. 1: Overall workflow of the proposed methodology

The experimentation part takes place on four dimensions. Initially, IoT devices enabled data acquisition for lung cancer diagnosis and the data are transmitted to the cloud server for diagnostic process. The data is preprocessed and filtered using Gaussian amended bilateral filter (GABF), and then the image is used for the segmentation process using improved U-net. Tumor features are extracted using stacked auto encoder model for reducing feature dimensionality issues. Finally hybrid deep learning model named as dilated depth-wise separable convolutional network assisted bidirectional long short term memory model is used to accurately

classify lung CT scans as cancerous or non-cancerous. Here the limitation is model parameters are didn't optimized this leads to produce complexity issue.

3.1 Pre-processing

The data used in this experiment is gathered from IoT devices that collects each patient's healthcare data which are then transmitted to the cloud server for authentication purposes. Pre-processing images are using well filtering methodology to enhance image size and efficiently stabilities images dissimilarity. The input images are gathered are pre-processed to unrestraint each dominances to encourage well outcomes. The filters are considered in this study that are bilateral filter (BF) and Gaussian Filter (GF). BF is refers as method utilizes for smoothens data through exchanging strength assessment of both pixel through weighted ordinary of strength values of bordering pixels and also it includes limitation, which are ineffectual process to eliminate high level noise. GF method is utilize for blurring images and removing noise, but it contain restriction like absence of adaptivity, building it a reduced amount of fit for tasks demanding detailed edge safeguarding or supervision non-gaussian noise. This limitation are overcome by combing BF and GF to create novel filtering method named as Gaussian Amended Bilateral Filter (GABF). The images are pre-processed using GABF [31], which helps to retain the valuable original image information. Input images and guidance are made non-identical for smoothening the images. The Gaussian blur process is denoted as,

$$V(c)=\sum_{cd} F_{p,q}^{G}(G) I_q \quad (1)$$

Where, the variant filtering linear translation approach is denoted as V and the input image is represented as I .The center location of the input image is denoted as c and the guidance filter is indicated as G . The kernel filter $F_{p,q}^{G}$ can be mathematically indicated as follows:

$$F_{p,q}^{G}=\frac{1}{N_f}\exp\left(-\frac{\|p-q\|^2}{F_k^2}\right) \quad (2)$$

Here, the normalizing factor and Gaussian spatial kernel is symbolized as N_f and $-\frac{\|p-q\|^2}{F_k^2}$ respectively. The improved Gaussian bilateral kernel is mathematically modelled as,

$$F_{p,q}^{GBF}(I,G^{-})=\frac{1}{N_f}\exp\left(-\frac{\|p-q\|^2}{\partial_x^2}\right)\exp\left(-\frac{\|I_p-G^{-}\|^2}{\partial_y^2}\right) \quad (3)$$

Here, $F_{p,q}^{GBF}$ indicates the filter kernel of positions p,q of the guidance image. The Gaussian spatial kernel and range kernel are expressed as $\left(-\frac{\|p-q\|^2}{\partial_x^2}\right)$ and $\left(-\frac{\|I_p-G^{-}\|^2}{\partial_y^2}\right)$ respectively. The filtered outcome of Gaussian bilateral filter (GBF) is expressed as,

$$V(c)=\sum_{cd} F_{p,q}^{GBF}(I,\overline{G}) I_q \quad (4)$$

However, GBF only works with local information which is not subjected to remove textures effectively. Hence, GABF is initiated to eliminate the textures and to preserve the edges of the image. This GABF comprises of global optimization and local regularization. Cross scale relative value utilizes local regularization for smoothening the gradients which can be determined by,

$$R=\left|\frac{D_{GABF}^{\partial 1}*\alpha S_{p,q}}{D_{GABF}^{\partial 2}*\alpha S_{p,q}}\right| \quad (5)$$

Here, the smoothening image is denoted as S, the gradient of smoothened image in p,q direction is indicated as $\alpha S_{p,q}$. Adaptable parameter is denoted as α. The small and large scale features are represented as $\left|D_{GABF}^{\partial 1}*\alpha S_{p,q}\right|$ and $\left|D_{GABF}^{\partial 2}*\alpha S_{p,q}\right|$ respectively. The global optimization function can be utilized to improve the outcomes of smoothened images.

$$Arg_S \min \|S-I\|_2^2 + k\left(\left\|\frac{D_{GABF}^{\partial 1}*\alpha S_{p,q}}{D_{GABF}^{\partial 2}*\alpha S_{p,q}}\right\|_1 + \left\|\frac{D_{GABF}^{\partial 1}*\alpha S_{p,q}}{D_{GABF}^{\partial 2}*\alpha S_{p,q}}\right\|_1\right) \quad (6)$$

Here to reduce the distance between the relativity outcome of GABF and the input image, the L1-norm fidelity is employed which is represented as $\|S-I\|_2^2$. The normalized outcome of GABF is modelled as,

$$\left\|\frac{D_{GABF}^{\partial 1}*\alpha S_{p,q}}{D_{GABF}^{\partial 2}*\alpha S_{p,q}}\right\|_1 = \left\|\frac{\left(D_{GABF}^{\partial 1}*\alpha S_p\right)^2}{\left(D_{GABF}^{\partial 2}*\alpha S_p\right)\left(D_{GABF}^{\partial 1}*\alpha S_p\right)}\right\|_1 \quad (7)$$

The regularization of GABF is estimated through equation (7). The GABF utilized L1 normalization as regularization technique which is more intricate when compared with L2 normalization. L1 normalization lacks differentiability at zero. Consequently, L2 regularization seems to be more prevalent choice in image processing tasks due to its smoothness and overall quality of filtered image. Henceforth, GABF is efficient for effective removal of digital noises and for attaining enhanced quality of input image.

3.2 Segmentation

The pre-processed images are fed into segmentation phase under improved U-Net model. Here, the U-Net model acts as a backbone for segmenting the images. U-Net has a simple structure and is able to accommodate minimum training sets and have the ability to extract the deep semantic information. U-Net [32,35] is very popular for medical image segmentation. However, U-Net failed to monitor the accurate location and boundaries of prostate glands. This leads to the possibility of including the area outside the prostate gland during segmentation. To obtain more accurate segmentation of the image, this research proposes an improved U-Net model with gated attention (GA) mechanism and conditional random fields. Compared with U-Net, improved U-Net model has better stability and segmentation effect. The architecture of improved U-Net is depicted as Figure 2.

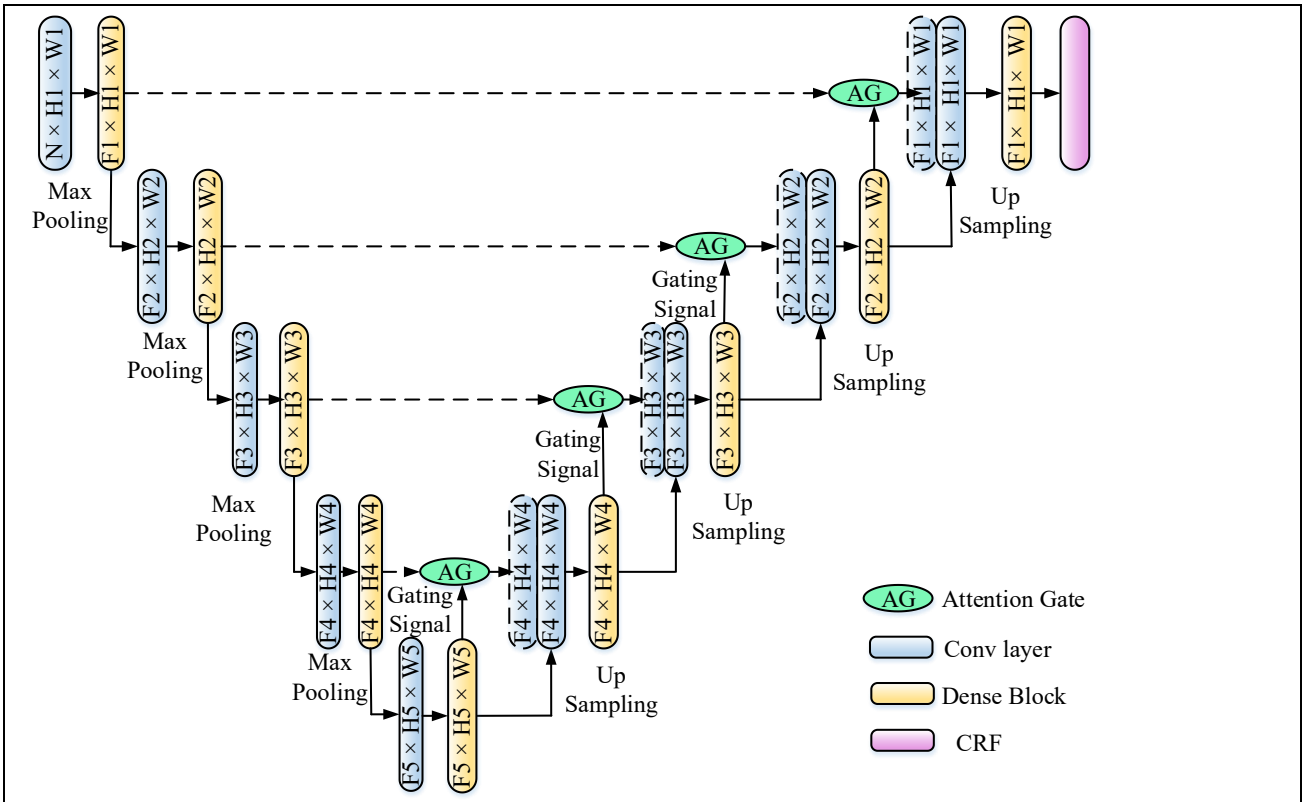

Fig. 2: Architecture of Improved U-Net model

The improved U-Net utilizes a de-convolution layer in the up sampling operations to restore the feature image to its original image [35]. In general, the issue of blurring the boundary may arises during segmentation process. To overcome the problem of blurred target of segmentation, the U-Net is combines with conditional random fields for accurate segmentation. This version utilizes fully connected conditional random fields for optimizing the segmented results. The improved U-Net model is structured with an encoder-decoder framework. In the encoder section, the input image is activated by two sets of 3×3 2D-convolutions with Rectified Linear Unit (ReLU) activation function followed by a maxpooling down-sampling function. After four sets of such convolutional and pooling blocks, the network enters the decoder phase. In addition to direct up sampling, the encoding's feature map also performs attention calculations from the encoder and integrate it into up sampling feature map. After such four up sampling blocks, a fully connected conditional random field is processed to attain the segmented output map. Compared to traditional U-Net decoders, the improved U-Net performs gated attention on features in the decoder which is connected to the encoder part. The obtained feature map contains different spatial information which helps the model to focus on specific target regions.

3.3 Feature extraction

The segmented images are exposed to feature extraction under Stacked Auto Encoder method. Auto encoder, contains neural network that acquires features. Encoding and decoding are two kind of function. In encoding part, segment data are conveyed to low-dimensional illustration interplanetary to abstract greatest related features, which are recorded backbone to input space in decoding part. The hidden layer are denoted to means of bottleneck later auto encoder are generally applied for solidity. The ReLU activation process are utilized in stacked auto-encoder. The rebuilding error are reduced among input-outcomes information, auto-encoders are absorb important features in informative data. The amount of outcomes layer neurons of auto encoder are same as amount of input layer neurons, Numerous layers of encoding and then an output layer of decoder are stacked to make SAE. Stacked auto encoder having two encoding and decoding layer are applied. Auto encoder are most generally trained such as stage of huge method, which input are simulated. An architecture of stacked auto encoder is displayed in Figure 3:

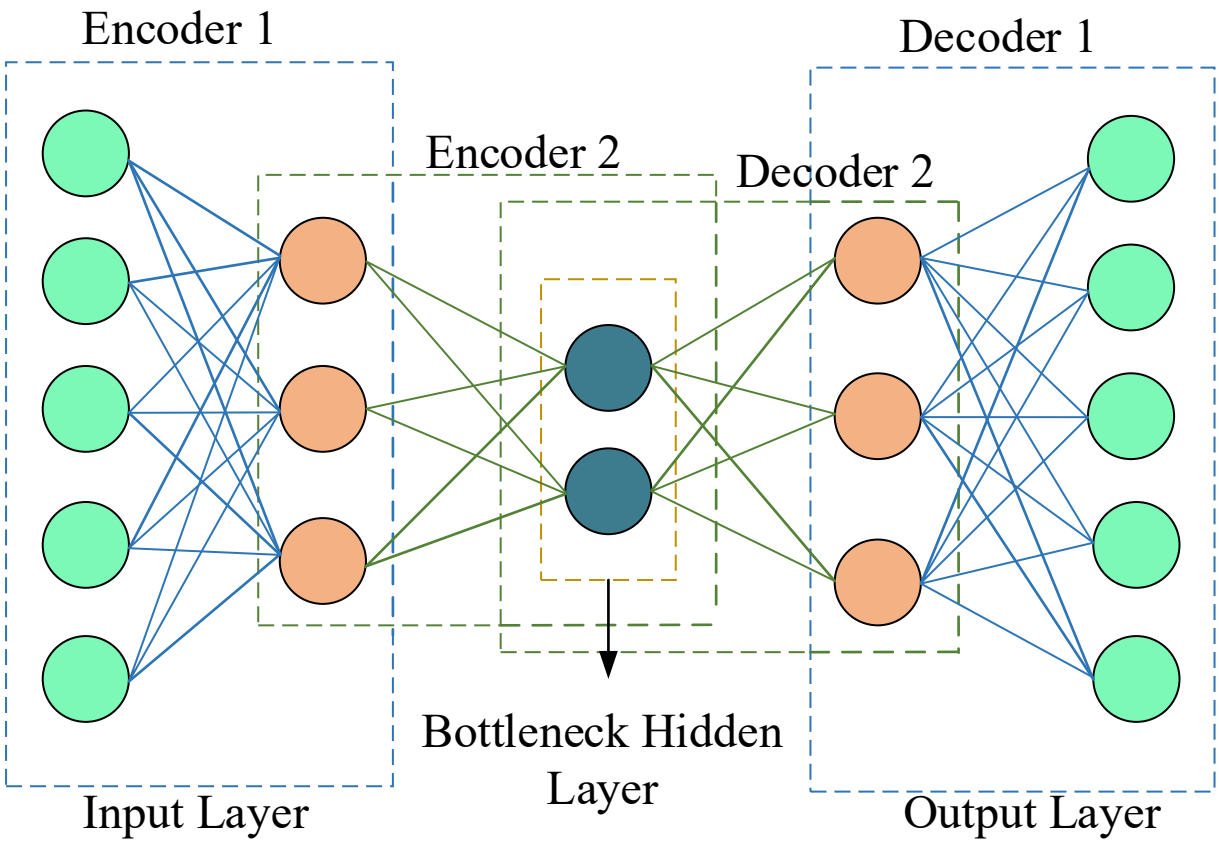

Fig. 3: Architecture of Stacked auto encoder for feature extraction

The structure of auto encoder method are embarrassed to bottleneck at midpoint, which input are reconstructed. The method produced fixed length by compressed version of input data at bottleneck. SAE architecture comprises numerous hidden layer, which allow it to represented difficult high-dimensional operations and abstract data features. Data that are stored in real space are take and converted into various space. For this specific part, input representation includes some terminated data, which conversion obtained are cleared. The real features are misplaced, but novel space contains novel features. The decoding layer are decode novel features into real form and check either encoder are correctly extracted data features or not. Particular of features are nominated although extra are forbidden by auto encoder. Therefore, this model purpose to regulate maximum accurate feature alteration. In this model includes two encoder and decoder are applied that may convert into real features into concentrated features excellently. SAE are exact supportive in on condition that decrease dimensionality issues. SAE might compress features to learn information from segmented images. SAE mainly contributed on shape and surface distortions. This not only focus on classification performance, but it might decrease computational costs.

3.4 Classification

After feature extraction, Dilated Depth-wise Separable Convolutional Network assisted Bidirectional Long-Short Term Memory (DDSW-Bi-LSTM) is used to classify lung tumor images. Here dilated convolutional and depth-wise separable convolutional [33] to enhance classification accuracy while maintaining method to be lightweight by adjusting hyper parameter. This division initial display knowledge of building joint model of dilated convolutional and depth-wise separable convolutional, which are utilized to build deep convolutional network. This method dilates both filter to occurred extra image data without enhancing total number of channels. The dilated filter are applied to convolve both input channel, and final filter are applied to joint outcomes of different convolutional channels. The architecture of DDSW method are illustrated as Figure 4.

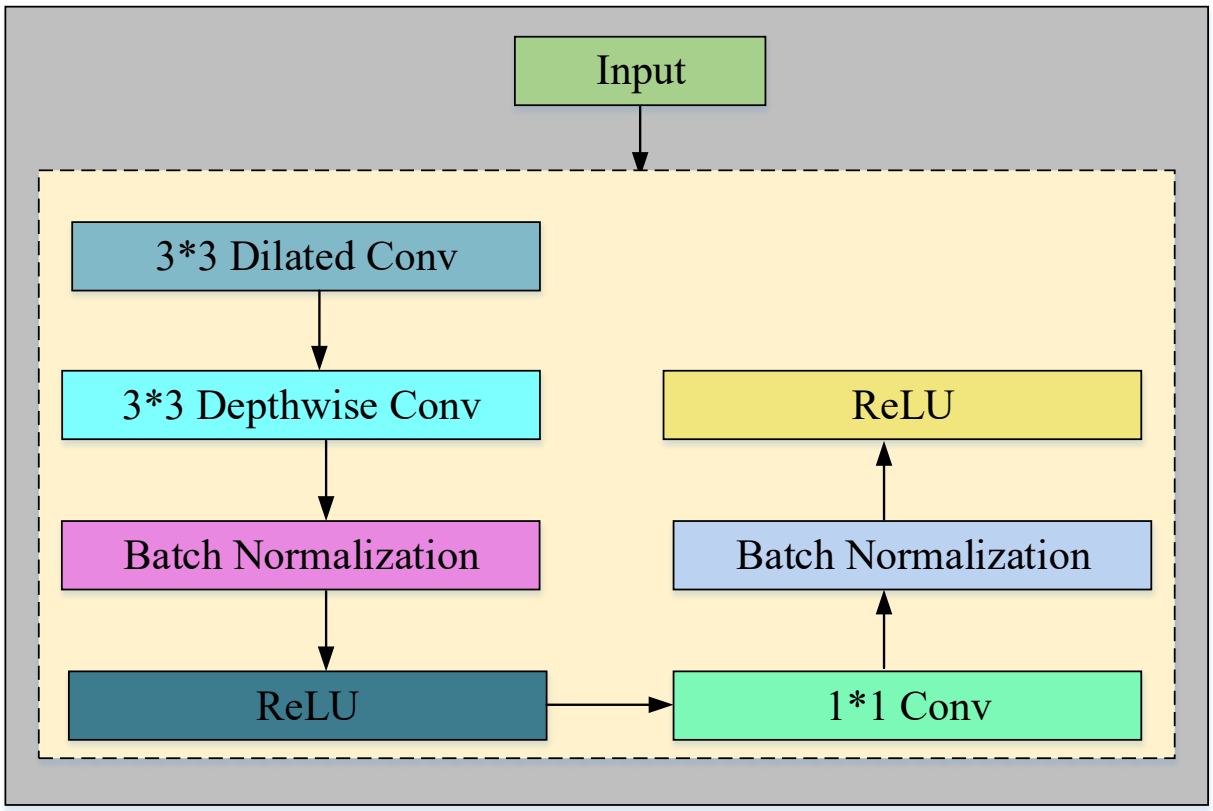

Fig. 4. Architecture of DDSW method.

By enhancing of receptive areas, it represent that both node included advanced semantic features, which might improving classification accuracy of channels. To factor guidance of various dilated convolution on method accuracy, it utilizes parameter to regulate extended of both dilated convolution. The relationship among receptive areas and actual filter size are represented as follows.

$$D=\left(T\times\lambda+\left(\lambda-1\right)\right)^2 \quad (8)$$

Where, D represent size of receptive area, T denoted size of beginning filter and λ represent dilated rate. The separable convolution operation are conceded out on attained dilated convolution filter. The amount of channels of both filters are 1 and image are convolved by using 1×1 size and convolutional channels. Then G denotes number of input channels, O number of output channels, $M_j\times M_j$ are height and width of dilated filter and $M_k\times M_k$ are represented as height and weight of input feature map. H_s denoted as total amount of parameter in modern convolutional functions.

$$H_s=M_j\times M_j\times G\times O\times M_k\times M_k \quad (9)$$

$$H_e=M_j\times M_j\times G\times M_k\times M_k+G\times O\times M_k\times M_k \quad (10)$$

Where, H_e ratio of separable convolutional to modern convolutional might be explored as:

$$\frac{H_e}{H_s}=\frac{1}{O}+\frac{1}{M_j^2} \quad (11)$$

Equation (11) display that evaluation might be decreased to $\frac{1}{O}+\frac{1}{M_j^2}$, which are compared to conventional convolutional function and provides lower computational difficulty. To escape gradient vanishing issues and haste up network training, which are utilized Batch Normalization (BN) and ReLU layer to create gradient superior, after presenting combined method. The method dilates 3 × 3 convolution kernel formerly applying both depthwise separable convolution. By dilated rate to acquire convolution kernel by superior receptive areas. The achieved 3×3 dilated convolution are utilized to both network of feature map, and before 1×1 convolution are utilized to association outcomes of channel convolution. Calculation BN layer and ReLU linear activation process both 1×1 convolution function are might be hasten training speed and increase generalization competence of network. LSTM model might be efficiently collect long-distance dependencies in time series data. The LSTM network contained three gate structures, which are effectively solved issues of gradient vanishing and exploding caused by RNN. LSTM have well detection behaviour over sometime by learning temporal features in lung classification data. Therefore LSTM might be transmit time sequence data about unit directionally and can't study from each directions concurrently. Here Bi-LSTM are utilized to classify bidirectional time sequence data, to enhance classification accuracy of lung tumor. Figure 5 represent BiLSTM architecture.

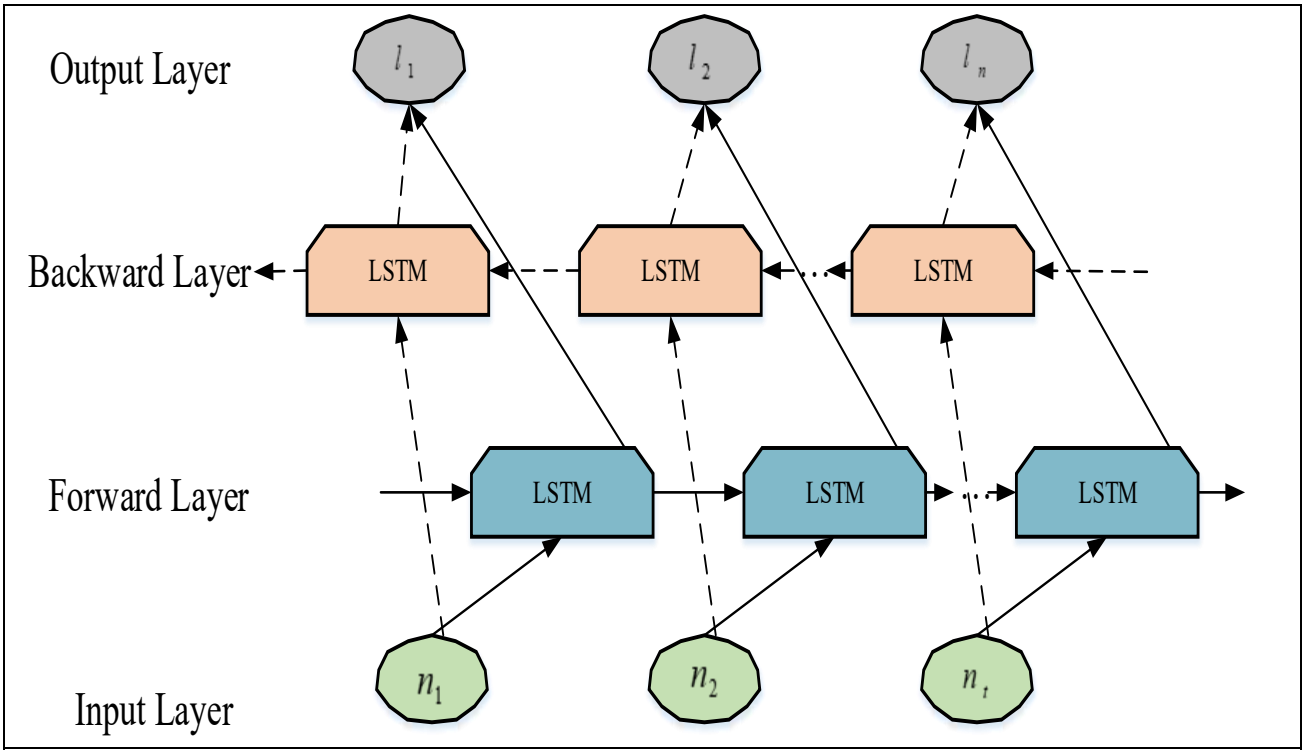

Fig. 5. Architecture for BiLSTM model

BiLSTM method are associated with forward LSTM and backward LSTM. Consuming input features of BiLSTM at time S are m_s. Hence forward output of LSTM at S are $\vec{g}_s$. Backward output features of LSTM at time S are $\overleftarrow{g}_s$. The last outcomes feature m_s of BiLSTM during at time S are occurred by combining $\vec{g}_s$ and $\overleftarrow{g}_s$. The modified function of BiLSTM are follow as, Figure 6 represent architecture for proposed DDWC-BiLSTM model.

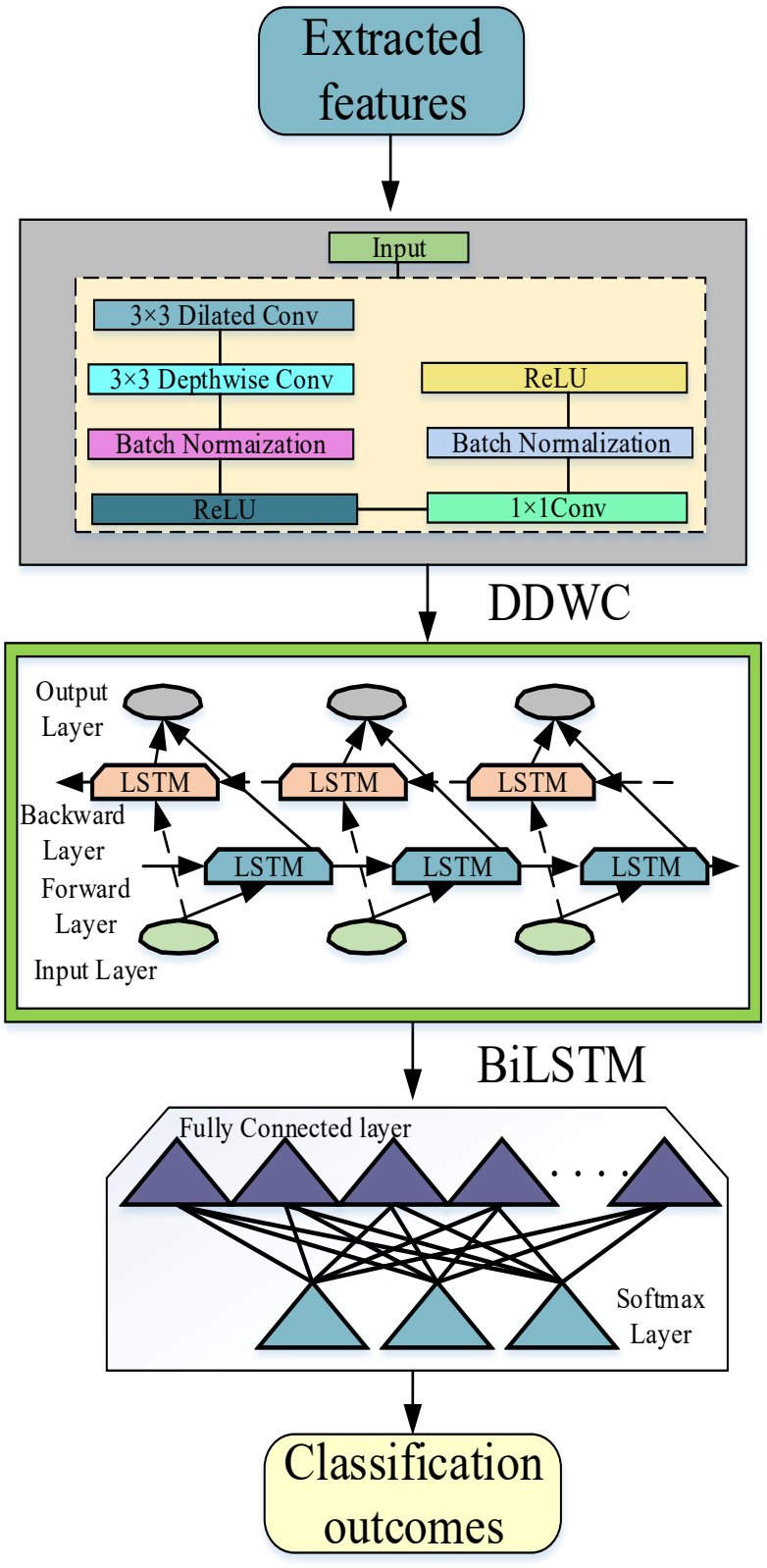

Fig. 6: Architecture for proposed DDWC-BiLSTM model

$$\begin{cases} \vec{g}_s = LSTM\left(m_s, \vec{g}_{s-1}\right) \\ \overleftarrow{g}_s = LSTM\left(m_s, \vec{g}_{s+1}\right) \\ m_s = \left[\vec{g}_s, \overleftarrow{g}_s\right] \end{cases} \quad (12)$$

Finally, superior feature demonstration that are integrated temporal and spatial addictions. The incorporated outcomes result of DDWC and Bi-LSTM are distributed by fully connected layer. This layer function illustrate as classifier, plotting incorporated features into particular classes such as lung tumor or normal. Here softmax activation function are utilized to produce possibilities applied for both class, which are superior possibility are selected as final classification class.

4. Results and analysis

This section provides the experimental results for proposed approach and compared it with previous models. Initially the details about system configuration and hyperparameters are described in Table 2 and 3.

Table 2: System configuration details

Specification	Details
Platform	Spyder (python 3.7.13)
System type	64-bit operating system, x64-based processor
GPU Processor	2.6 GHz 6-core Intel core i7
Graphics	Radeon Pro 560X 4 GB Intel UHD Graphics 630 1536 MB

Table 3: Hyperparameters details

Hyperparameters	Values
Optimizer	Adam
Number of units	64
Activation	Softmax
Batch size	32
Dropout	0.2

4.1 Dataset description

This section deliver Dataset description are given in follow as,

Dataset 1:

Lung Tumor Segmentation dataset is consists of 62 images and masks files, which all files contains 15,208 images.

Dataset link: https://www.kaggle.com/datasets/rasoulisaeid/lung-cancer-segment

Dataset 2:

Medical Segmentation Decathlon (MSD) [34] is group of dataset particularly created to test toughness of segmentation method through wide-ranging structural sections and imaging environments. All MSD dataset are preserved as different process, offering distinctive limitations that highlight segmentation presentation applied for exact areas of interest. In this research, MSD_Lung dataset are applied for analysis. This dataset includes 63 scans data, which all scan files data contains 35,314 images from patient by non-small cell lung cancer. It objective segment of lung tumors, characterized by single label.

Dataset link: http://medicaldecathlon.com/

4.2 Performance metrics

Mathematical expression for performance metrics is displayed in Table 4.

Table 4: Mathematical expression for performance metrics

Metrics	Expression
Accuracy	$Accuracy = \frac{(TP + TN)}{(TP + FP) + (FN + TN)}$
Precision	$\Pr ecision = \frac{TP}{(TP + FP)}$
Recall/Sensitivity	$\mathrm{Re}\, call / Sensitivity = \frac{TP}{TP + FN}$
F1-score	$F1Score = 2 \times \frac{(\Pr ecision \times \mathrm{Re}\, call)}{\Pr ecision + \mathrm{Re}\, call}$
Dice	$Dice\, Score = 2 \times \frac{(\Pr ecision \times \mathrm{Re}\, call)}{\Pr ecision + \mathrm{Re}\, call}$
Specificity	$Specificity = \frac{TN}{(TN + FP)}$
IoU	$IoU = \frac{TP}{(TP + FP + FN)}$
MSE	$MSE = \frac{1}{n}\sum_{i=1}^{n}(\hat{y}_l - y_i)^2$
RMSE	$RMSE = \sqrt{\frac{1}{n}\sum_{i=1}^{n}(\hat{y}_l - y_i)^2}$

Form the Table 4, TP, TN, FP and FN are describes true positive, true negative, false positive, and false negative respectively. Also $\hat{y}_l$ defines predicted value for i^{th} data point, n stands for number of observations.

4.3 Performance evaluation

This section shows the performance of proposed and previous models in terms of graphical representation for both datasets.

4.3.1 For Kaggle dataset

4.3.1.1 Segmentation results

Some segmentation performance results for proposed and other models are evaluated and compared in this section. Figure 6 shows performance comparison of (a) Dice, (b) IoU, (c) sensitivity, and (d) specificity.

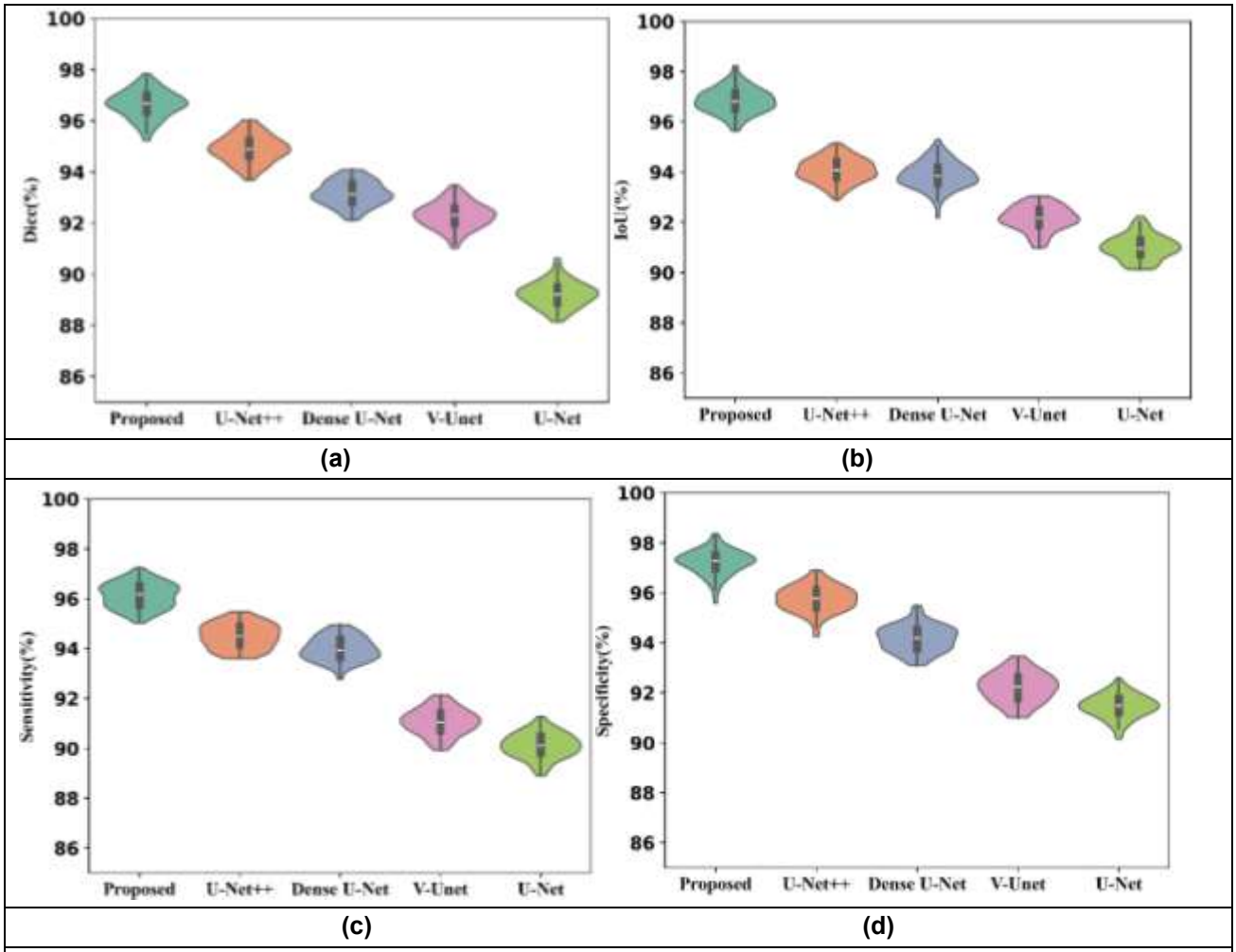

Fig. 7. Performance comparison of (a) Dice, (b) IoU, (c) sensitivity, and (d) specificity

Compare to previous models proposed model attain effective results in terms of dice, IoU, sensitivity, and specificity. Figure 7 (a) evaluates dice performance, here proposed approach attain high performance that is 96.54%. IoU performance of proposed approach is 96.85%, which is observed from Figure 7 (b). Proposed approach sensitivity of 96.12% that is shown in Figure 7(c). Figure 7 (d) illustrates specificity performance of proposed approach is 97.25%. Table 5 shows segmentation performance comparison of proposed and previous models.

Table 5: Segmentation performance comparison of proposed and previous models

Model	IoU	Dice	Sensitivity	Specificity
Proposed	**0.9685**	**0.9654**	**0.9612**	**0.9725**
U-Net++	0.9415	0.9484	0.9451	0.9581
Dense U-Net	0.9385	0.9317	0.9396	0.9425
V-Unet	0.9213	0.9222	0.9102	0.9212
U-Net	0.9086	0.8923	0.9023	0.9142

4.3.1.2 Classification results

Here the proposed classifier results is evaluated and compared with some previous classifier namely CNN, RNN, LSTM and DSC. Figure 8 represents performance comparison of (a) accuracy, (b) precision, (c) specificity (d) F1-score.

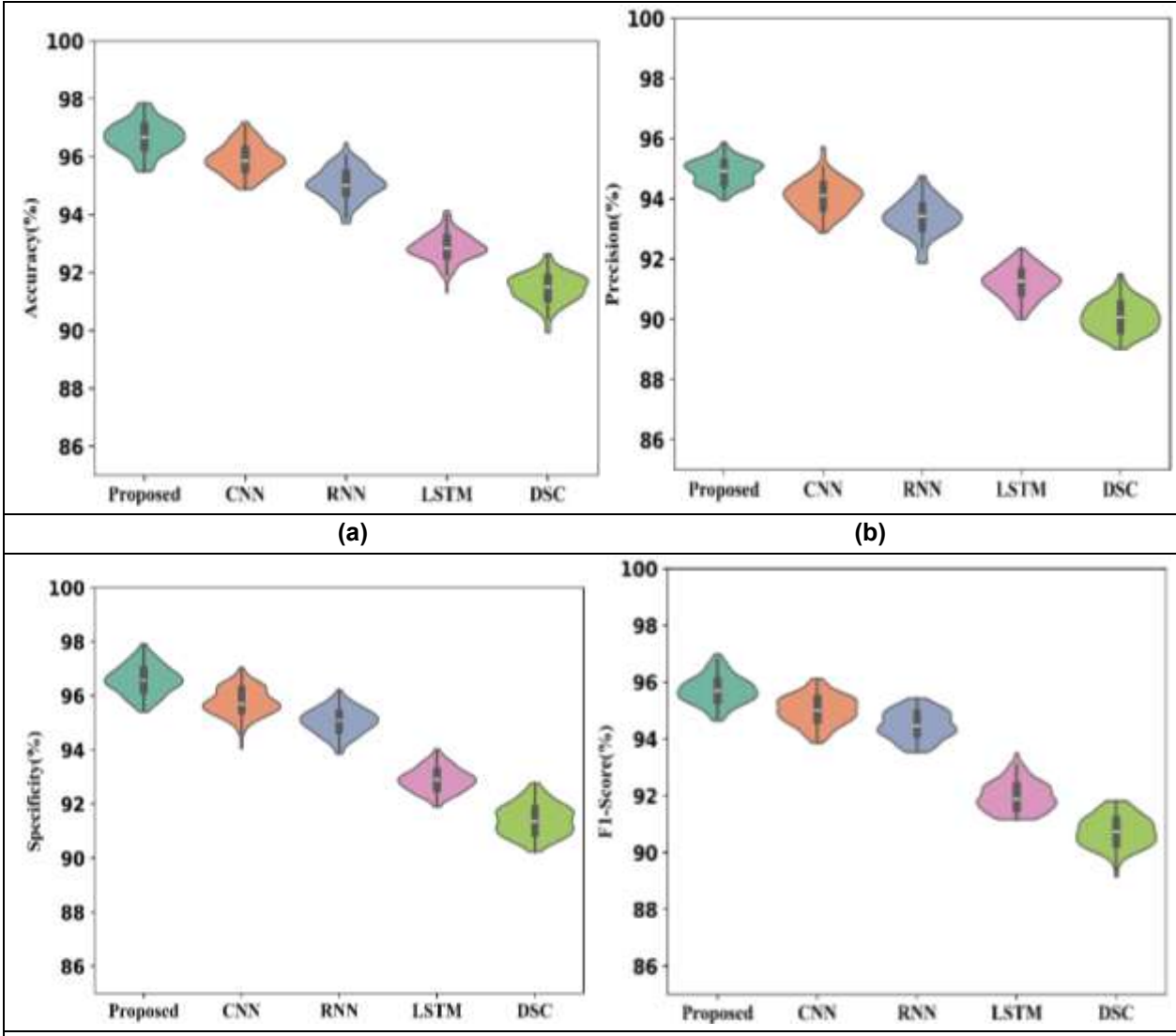

Fig. 8: Performance comparison of (a) accuracy, (b) precision, (c) specificity (d) F1-score.

The graphs compare the proposed and previous classifiers' performance in terms of various performance metrics like accuracy, precision, recall and F-measure. Here, the proposed approach attains an accuracy of 96.62%, Precision of 94.87%, specificity of 96.54% and 95.79% of F1-score. Compare to the proposed approach, previous classifiers attain low performance results due to misclassification. High accuracy of the proposed classifier indicates that the proposed approach accurately predicts tumor classes and produces less false rates. Figure 9 represents the performance analysis of (a) MAE, (b) MSE and (c) RMSE.

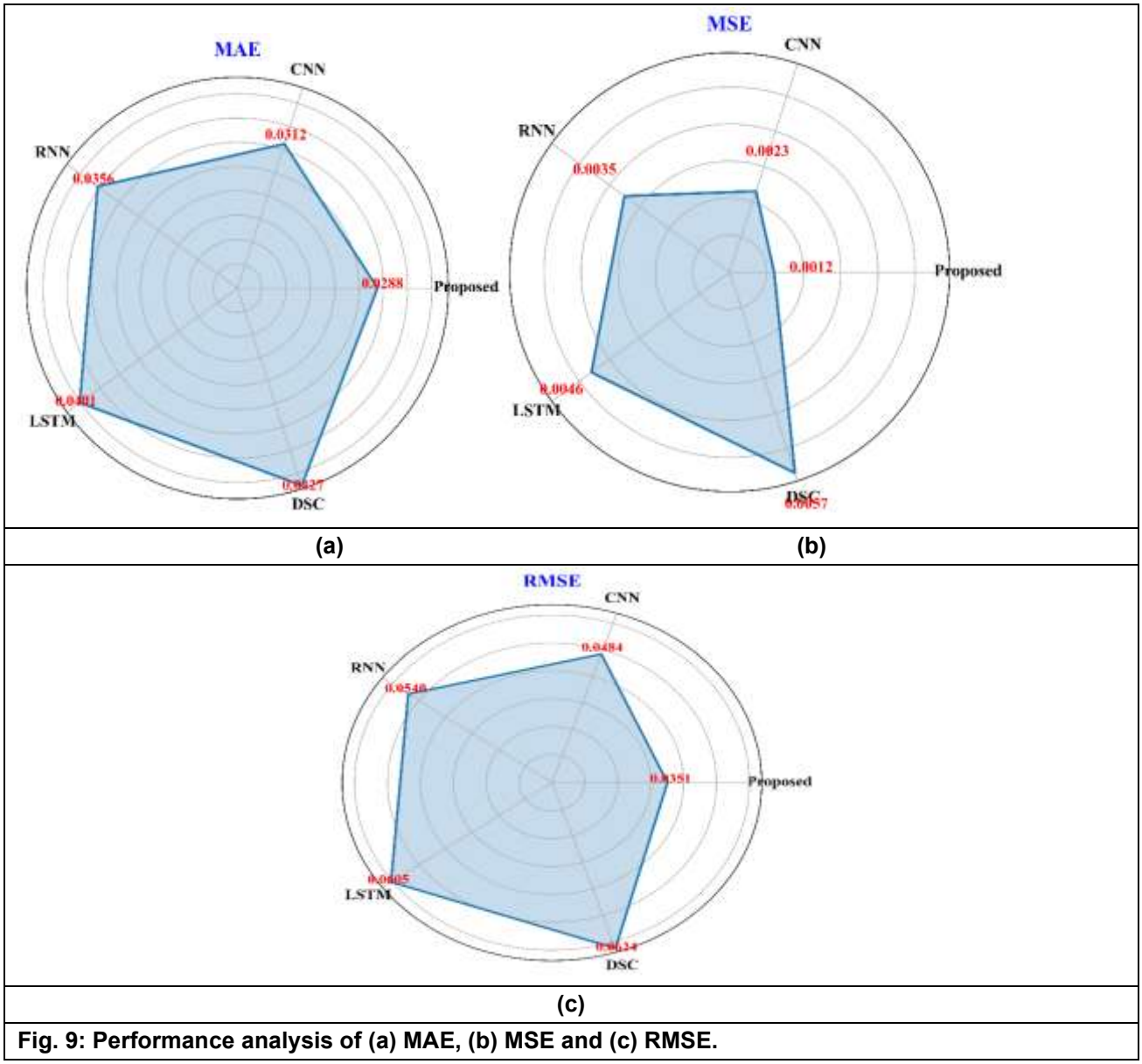

(a) (b)

(c)

Fig. 9: Performance analysis of (a) MAE, (b) MSE and (c) RMSE.

Compare to propose method previous method produces high error results. MAE performance of the proposed approach is 0.0288, which is given in Figure 9 (a). The MSE score is estimated and deployed in Figure 9 (b) to show the error score that occurred in the proposed model is 0.0112. The proposed approach produce 0.0351 RMSE in lung tumor classification is given in Figure 9 (c). Table 6 shows classification performance comparison of proposed and previous models.

Table 6: Classification performance comparison of proposed and previous models.

Model	Accuracy	Precision	F1-Score	Specificity	MSE	RMSE	MAE
Proposed	**0.9662**	**0.9487**	**0.9579**	**0.9654**	**0.0012**	**0.0351**	**0.0288**
CNN	0.9584	0.9409	0.9497	0.9578	0.0023	0.0484	0.0312
RNN	0.9515	0.9337	0.9443	0.9511	0.0035	0.054	0.0356
LSTM	0.9288	0.9126	0.9203	0.9288	0.0046	0.0605	0.0401
DSC	0.9146	0.9005	0.9071	0.914	0.0057	0.0624	0.0427

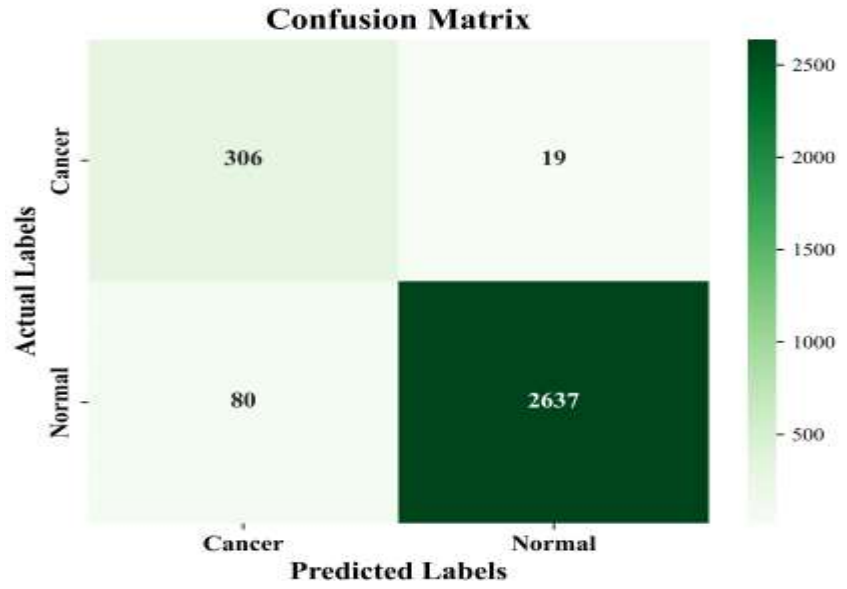

Fig. 10: Confusion matrix analysis

Figure 10 described confusion matrix results for kaggle dataset using proposed classifier. 2637 and 306 normal and cancer classes are correctly predicted. Meanwhile 80 from normal and 19 from cancer classes are wrongly predicted classes in kaggle dataset. Figure 11 compares the accuracy and loss of the training and testing stages. From Figure 11 (a), it is observed that the proposed model has the best training convergence and produces superior training accuracy. For both training and testing high accuracy values are attained by the proposed approach. Figure 11 (b) displays the model's loss curve. As the number of epochs rises, the value of the loss falls. The suggested method offers better accuracy with less loss analysis because it introduces multiple learning stages and attention mechanisms at the beginning.

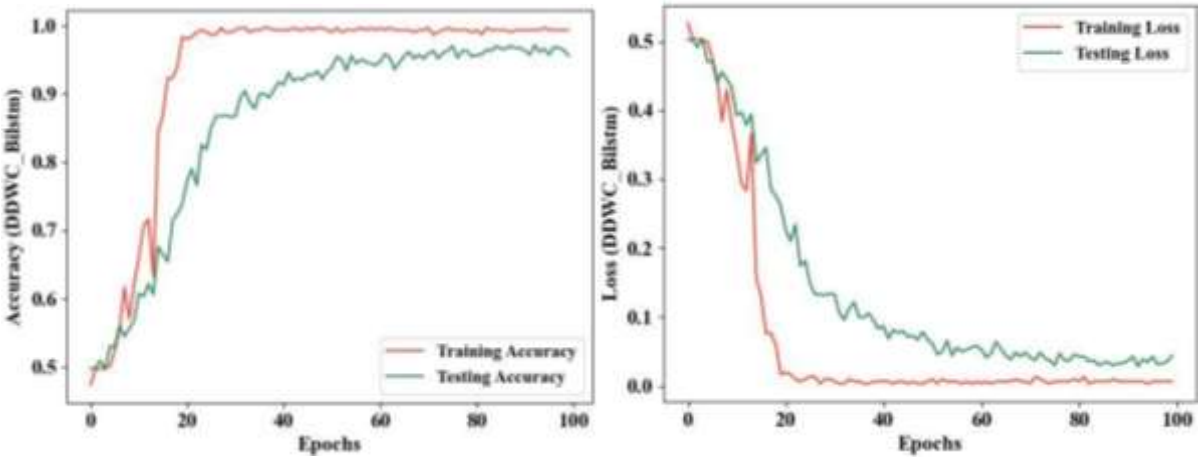

(a) **(b)**

Fig. 11: (a) Accuracy and (b) loss during training and testing

4.3.2 For Medical Segmentation Decathlon lung dataset

4.3.2.1 Segmentation results

This section evaluates the performance of the proposed method with previous segmentation models such as U-Net, V-Unet, Dense U-Net, and U-Net++. Figure 11 shows performance comparison of (a) dice, (b) IoU, (c) sensitivity, and (d) specificity.

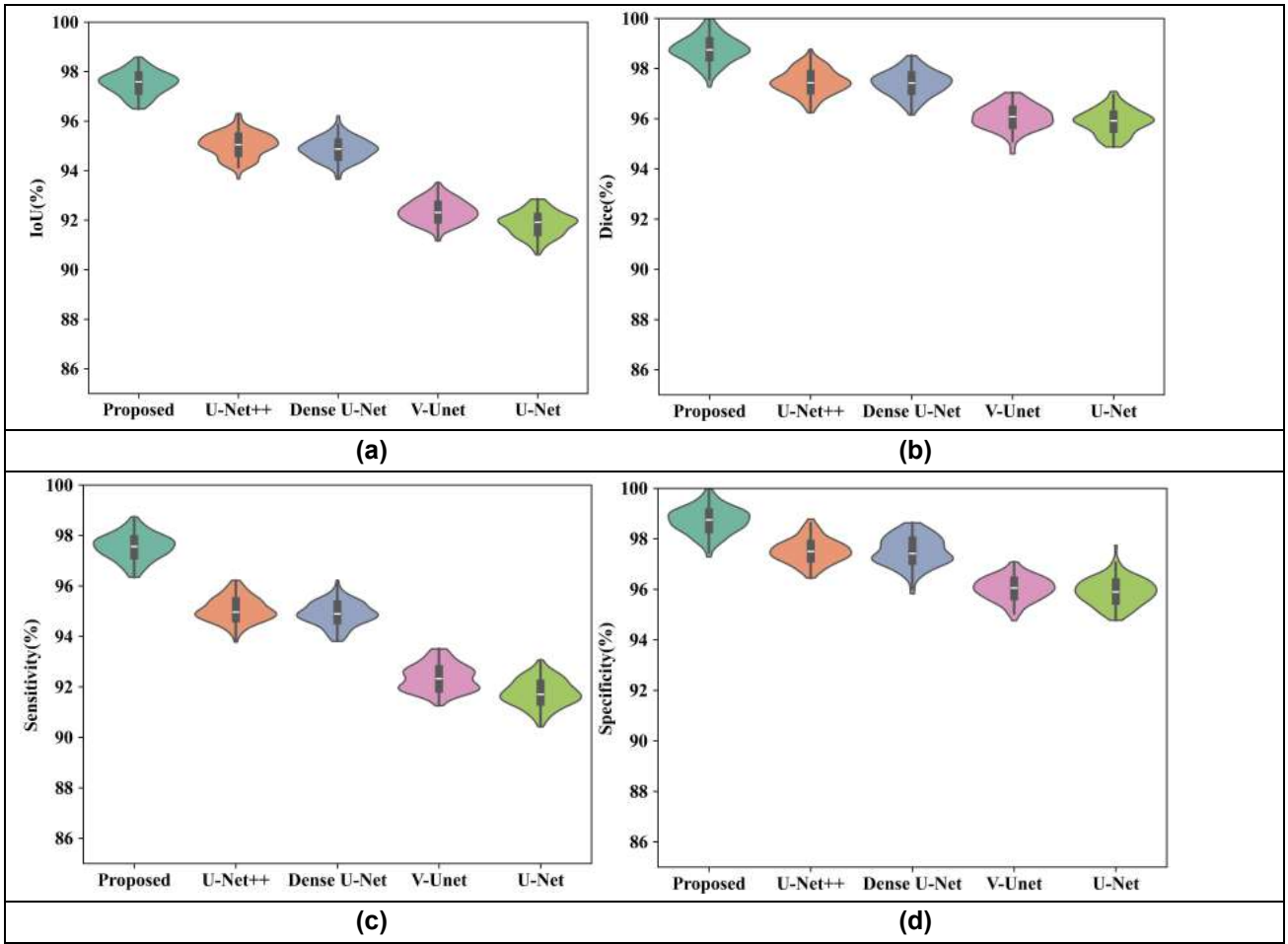

Fig. 12: Performance comparison of (a) dice, (b) IoU, (c) sensitivity, and (d) specificity.

The graphs shows comparison in terms of dice, IoU, sensitivity and specificity. In Figure 12 (a) proposed method attain 97.46% dice score, while other models produce less than 97%. IoU of proposed approach is 98.72%, which is given in Figure 12 (b). Sensitivity of proposed approach is 97.46% that is shown in Figure 12 (c). Figure 12 (d) shows that specificity of proposed approach is 98.72% while other models are obtained less than 98%. Table 7 shows segmentation performance comparison of proposed and previous models.

Table 7: Segmentation performance comparison of proposed and previous models.

Model	IoU	Dice	Sensitivity	Specificity
Proposed	0.9746	0.9872	0.9746	0.9872
U-Net++	0.9505	0.9747	0.9505	0.9747
Dense U-Net	0.9486	0.9744	0.9486	0.9744
V-Unet	0.9237	0.9605	0.9237	0.9605
U-Net	0.9181	0.9593	0.9181	0.9593

4.3.2.2 Classification results

Here the proposed technique is compared with previous classifiers like CNN, RNN, LSTM, and DSC. Figure 13 shows performance comparison of (a) accuracy, (b) precision, (c) recall (d) F1-Score.

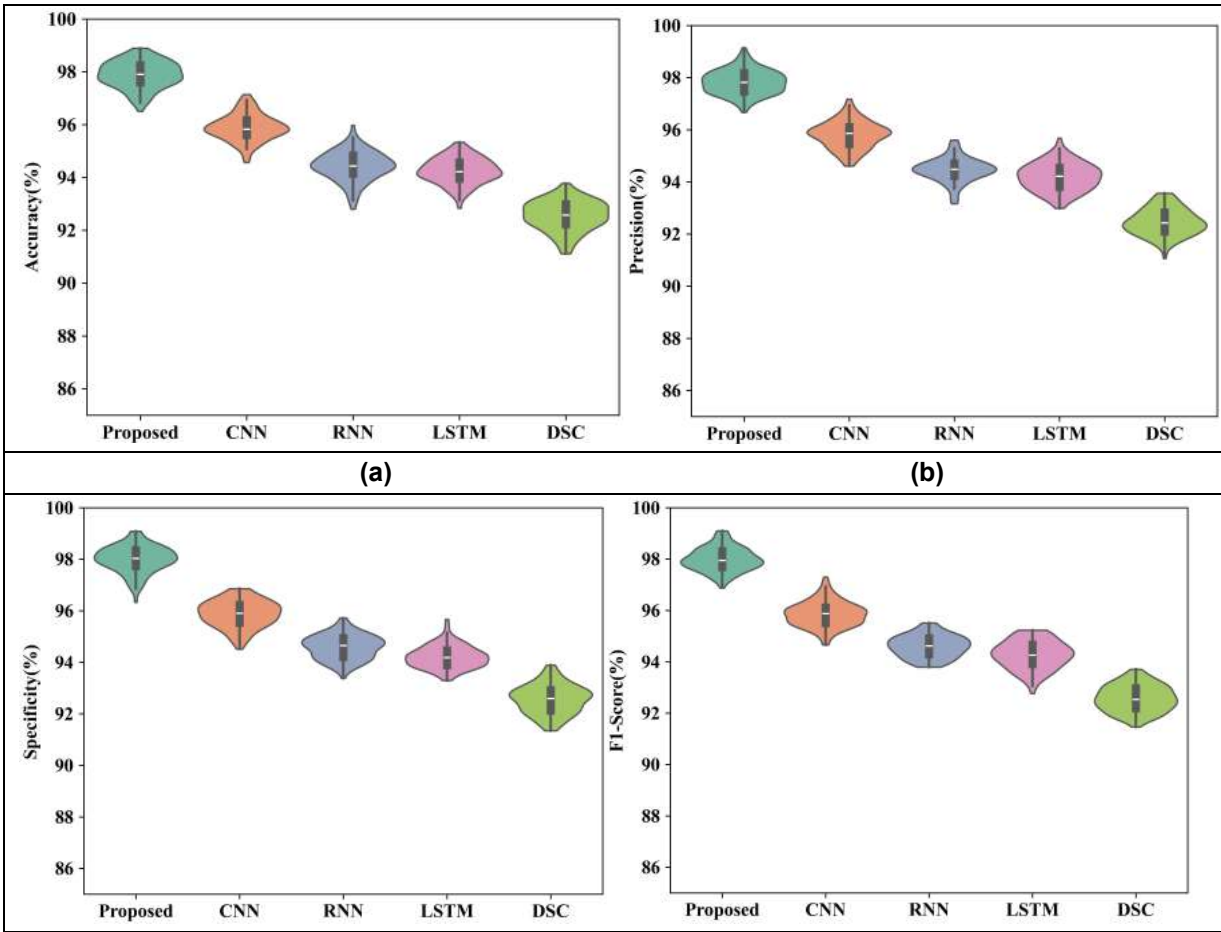

Fig. 13. Performance comparison of (a) accuracy, (b) precision, (c) specificity (d) F1-Score.

The graphs compares various performance like accuracy, precision, recall and F-measure for proposed and previous methods. Figure 13 (a) describes accuracy analysis, here the proposed approach attain high performance that is 97.93%. Proposed classifier attain 97.93% precision performance that is shown in Figure 13 (b). Specificity performance of proposed approach is 97.93%, which is illustrated in Figure 13 (c). Figure 13 (d) shows F1-Score performance, here the proposed approach produce 97.93%.

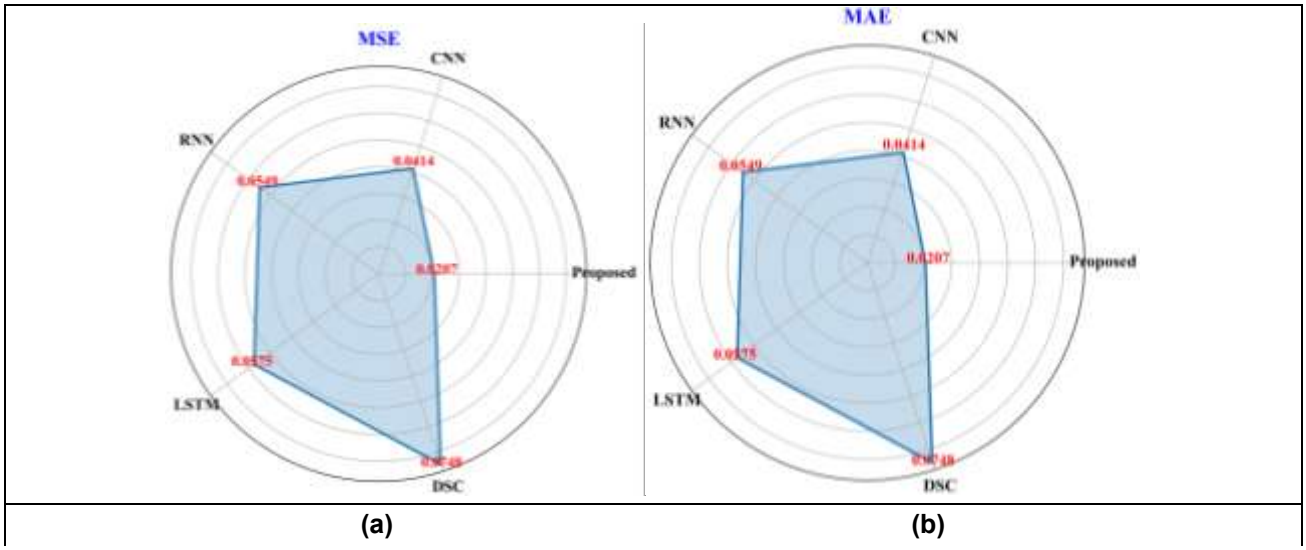

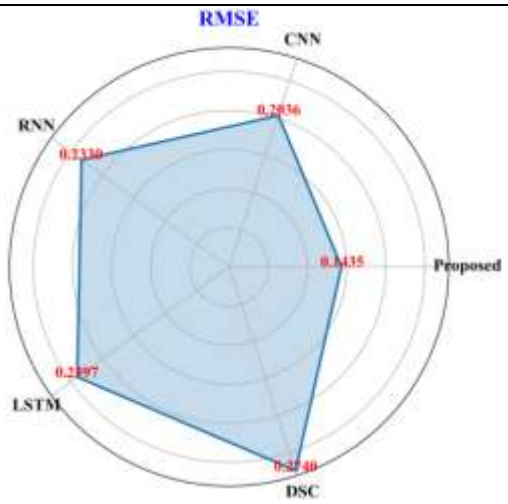

(c)

Fig. 14: Performance analysis of (a) MSE, (b) RMSE and (c) MAE

Here error performance comparison like MAE, MSE and RMSE are illustrated. Proposed approach attain 0.0207 MSE, 0.1435 RMSE, and 0.0207 MAE results respectively. Compare to previous models proposed approach attain less error metrics due to using transfer learning model in feature extraction stage. Previous classifiers takes more time for training and absence of feature extraction and selection stages leads to attain high error. Table 8 shows classification performance comparison of proposed and previous models.

Table 8: Classification performance comparison of proposed and previous models.

Model	Accuracy	Precision	F1-Score	Specificity	MSE	RMSE	MAE
Proposed	**0.9793**	**0.9793**	**0.9793**	**0.9793**	**0.0207**	**0.1435**	**0.0207**
CNN	0.9586	0.9586	0.9586	0.9586	0.0414	0.2036	0.0414
RNN	0.9451	0.9451	0.9451	0.9451	0.0549	0.233	0.0549
LSTM	0.9425	0.9425	0.9425	0.9425	0.0575	0.2397	0.0575
DSC	0.9252	0.9252	0.9252	0.9252	0.0748	0.274	0.0748

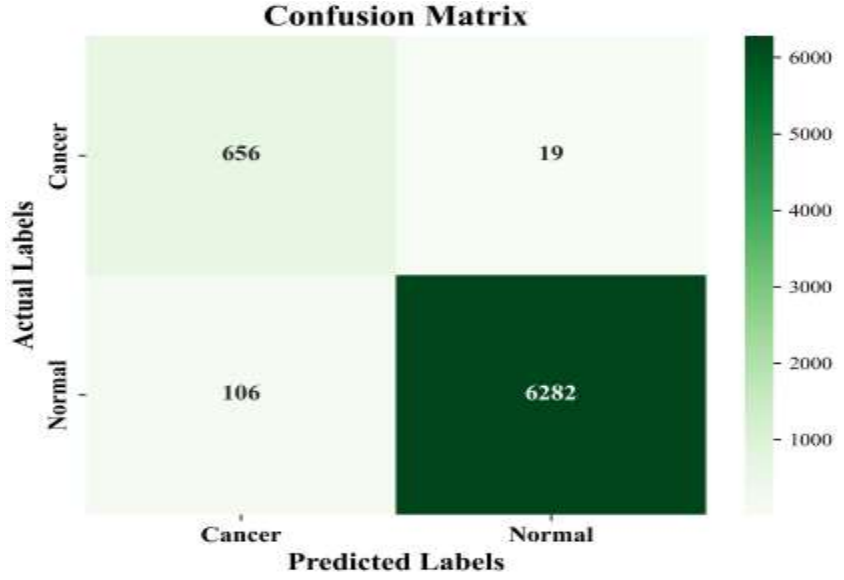

Fig. 15: Confusion matrix

In Figure 15 shows confusion matrix for Medical Segmentation Decathlon lung dataset using proposed model. Predicted classes represented as the number that is 6282 normal and 656 cancer. Then 19 images from cancer and 106 images form normal classes is wrongly predicted. Figure 16 mentions the accuracy and loss comparison of the training and testing stages.

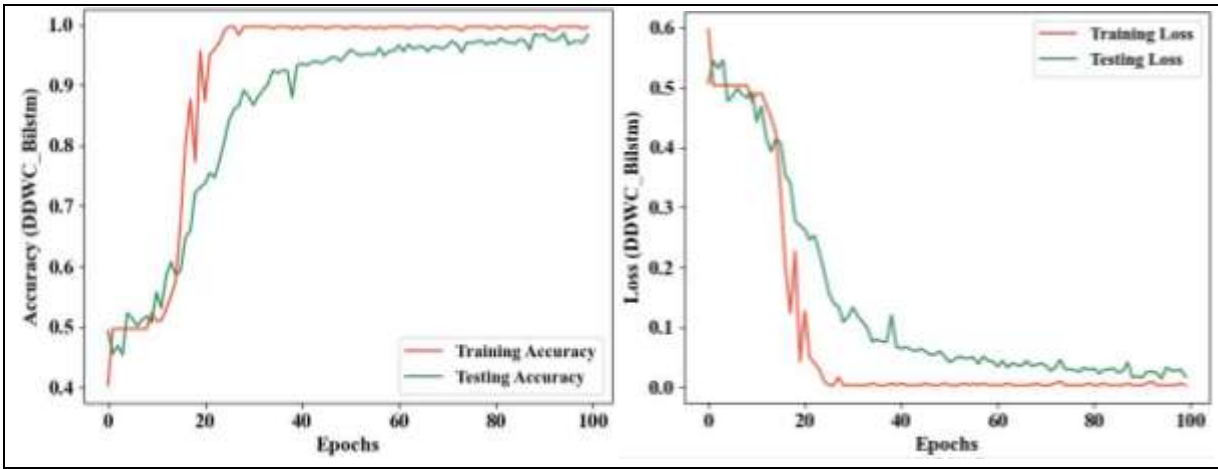

(a) (b)

Fig. 16: Comparison analysis of accuracy and loss curve (a) accuracy and (b) loss

During training and testing, the accuracy and loss of the classifiers are evaluated by modifying the size of the epochs. The accuracy level stabilizes in the 80–100 epoch range. The testing loss indicates that the proposed segmentation model reduces loss. The epoch size has been adjusted to provide an estimate for the curve analysis. The same level of accuracy is achieved with both the training and test samples.

4.4 Visualized outcomes

This section provides some sample images from both datasets. Figure 17 displays visualized outcomes for kaggle dataset. Figure 18 displays visualized outcomes for Medical Segmentation Decathlon lung dataset.

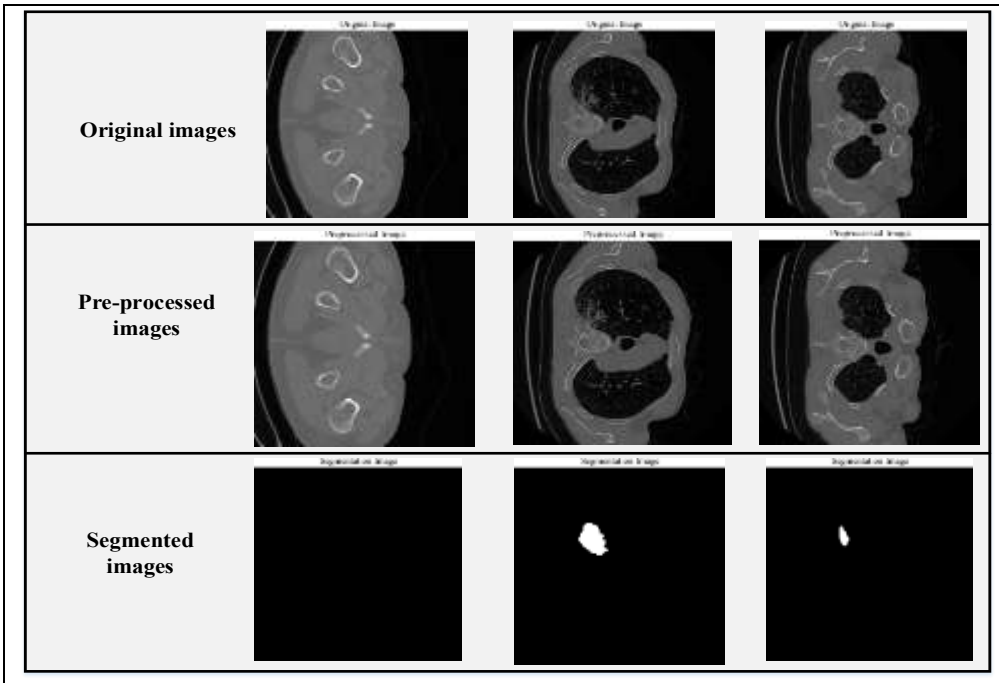

Fig. 17: Visualized outcomes for kaggle dataset

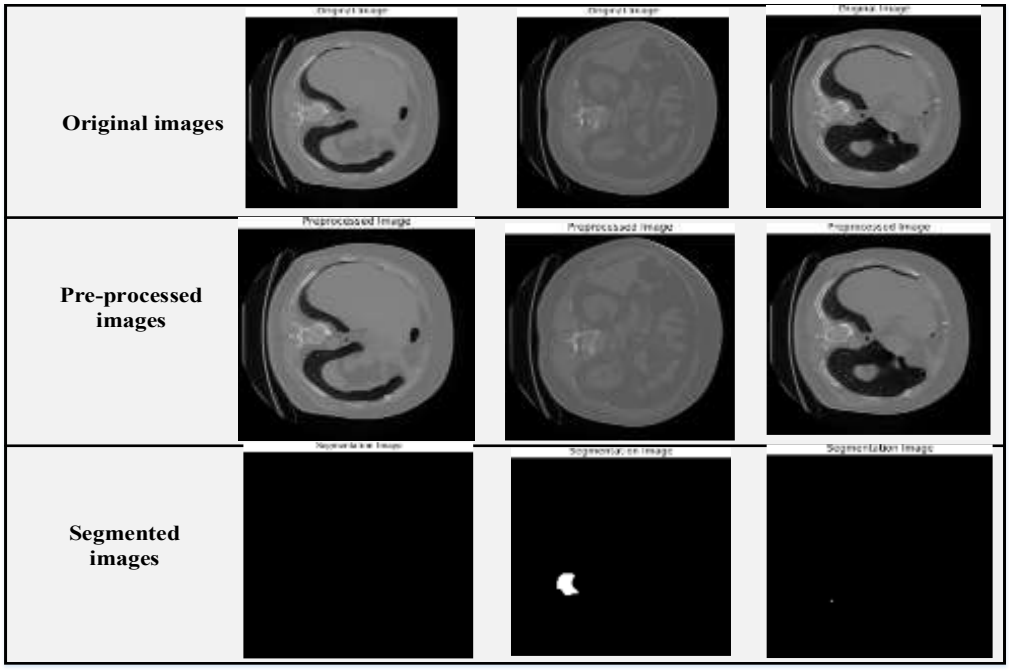

Fig. 18: Visualized outcomes for Medical Segmentation Decathlon lung dataset

4.5 Statistical analysis

This section evaluates the statistical analysis to define the significance and accuracy of the results attained by the proposed approach in the lung tumor detection system.

4.5.1 Confidence intervals

Confidence intervals (CI) offer valuable insights into the precision of the proposed approach accuracy estimates. This section computes confidence intervals around described accuracies to quantify the range within which the true accuracy of the model is likely to fall. For instance, with a confidence level of 95%, the CI is calculated as,

$$\mathrm{CI} = \mathrm{accuracy} + \_C * \sqrt{\frac{\mathrm{accuracy} * (1 - \mathrm{accuracy})}{\mathrm{Total\ samples}}} \qquad (13)$$

Where, C stands for critical value from standard normal distribution corresponding to the chosen confidence level.

4.5.2 P-value for statistical significance

This section computes p-values using suitable statistical tests like t-test or ANOVA to determine if the improvements in accuracy are statistically significant. The null hypothesis H0 assumes no significant difference between the accuracies of the proposed method and existing methods, while alternative hypothesis H1 suggests a significant difference.

A low p-value (typically<0.05) defines that the detected improvements in accuracy are unlikely to occur by random chance and are thus statistically significant.

4.6 Generalization and clinical implications

Model robustness and generalization

Generalization indicates the ability of the DL model to perform well, not only on the training dataset but also on unseen data from similar distributions. In the context of lung tumor using hybrid DL, generalization is crucial

for practical clinical deployment. This section evaluates the robustness and generalization capabilities of the proposed system's cross-validation on independent datasets. This process helps to validate the model's performance in real-world scenarios beyond the training data.

Clinical Implications

The successful deployment of DL models in clinical settings requires careful consideration of different factors beyond accuracy metrics. These features include model interpretability, explainability of predictions, regulatory compliance, integration with the existing clinical workflows, and ethical considerations regarding patient data privacy and security. The proposed study acknowledges these difficulties and highlights the importance of model explainability in medical decision making.

5. Conclusion

This study explores the use of hybrid DL models for lung tumor diagnosis with improved U-Net model. Proposed approach consists of four terms that are data acquisition, data processing, feature extraction and lung tumor classification. Here for segmentation improved U-net model is used segment the tumor region from the surrounding lung tissue. From the segmented image relevant features are extracted by using stacked auto encoder model. This technique helps reduce the dimensionality of the feature space, making subsequent analysis more efficient. Lastly, hybrid DL model named as DDWC-BiLSTM used for classifying cancer and normal classes. The evaluation of proposed approach is conducted on two datasets namely kaggle and Medical Segmentation Decathlon lung dataset. Proposed technique obtain an accuracy of 96.62% and 97.86% for kaggle and Medical Segmentation Decathlon lung datasets respectively. Here the limitation is model parameters are didn't optimized this leads to produce complexity issue. Future novel hybrid optimized model will be used to solve this issue.

References

1. Thilakarathne, Navod Neranjan, Mohan Krishna Kagita, and Thippa Reddy Gadekallu. "The role of the internet of things in health care: a systematic and comprehensive study." *Available at SSRN 3690815* (2020).
2. Asghari, Parvaneh, Amir Masoud Rahmani, and Hamid Haj Seyyed Javadi. "A medical monitoring scheme and health-medical service composition model in cloud-based IoT platform." *Transactions on Emerging Telecommunications Technologies* 30, no. 6 (2019): e3637.
3. Alshehri, Fatima, and Ghulam Muhammad. "A comprehensive survey of the Internet of Things (IoT) and AI-based smart healthcare." *IEEE Access* 9 (2020): 3660-3678.
4. Pradhan, Bikash, Saugat Bhattacharyya, and Kunal Pal. "IoT-based applications in healthcare devices." *Journal of healthcare engineering* 2021 (2021): 1-18.
5. Al-Khafajiy, Mohammed, Thar Baker, Carl Chalmers, Muhammad Asim, Hoshang Kolivand, Muhammad Fahim, and Atif Waraich. "Remote health monitoring of elderly through wearable sensors." *Multimedia Tools and Applications* 78, no. 17 (2019): 24681-24706.
6. Aceto, Giuseppe, Valerio Persico, and Antonio Pescapé. "Industry 4.0 and health: Internet of things, big data, and cloud computing for healthcare 4.0." *Journal of Industrial Information Integration* 18 (2020): 100129.
7. Liu, Ying, Lin Zhang, Yuan Yang, Longfei Zhou, Lei Ren, Fei Wang, Rong Liu, Zhibo Pang, and M. Jamal Deen. "A novel cloud-based framework for the elderly healthcare services using digital twin." *IEEE access* 7 (2019): 49088-49101.
8. Carioli, G., M. Malvezzi, P. Bertuccio, P. Boffetta, F. Levi, C. La Vecchia, and E. Negri. "European cancer mortality predictions for the year 2021 with focus on pancreatic and female lung cancer." *Annals of Oncology* 32, no. 4 (2021): 478-487.
9. Cao, Wei, Hong-Da Chen, Yi-Wen Yu, Ni Li, and Wan-Qing Chen. "Changing profiles of cancer burden worldwide and in China: a secondary analysis of the global cancer statistics 2020." *Chinese medical journal* 134, no. 07 (2021): 783-791.

10. Corrales, Luis, Rafael Rosell, Andres F. Cardona, Claudio Martin, Zyanya Lucia Zatarain-Barron, and Oscar Arrieta. "Lung cancer in never smokers: The role of different risk factors other than tobacco smoking." *Critical reviews in oncology/hematology* 148 (2020): 102895.
11. Manoharan, Dr Samuel, and A. Sathesh. "Early diagnosis of lung cancer with probability of malignancy calculation and automatic segmentation of lung CT scan images." *Journal of Innovative Image processing* 2, no. 4 (2020): 175-186.
12. Santos, Marcel Koenigkam, José Raniery Ferreira Júnior, Danilo Tadao Wada, Ariane Priscilla Magalhães Tenório, Marcello Henrique Nogueira-Barbosa, and Paulo Mazzoncini de Azevedo Marques. "Artificial intelligence, machine learning, computer-aided diagnosis, and radiomics: advances in imaging towards to precision medicine." *Radiologia brasileira* 52 (2019): 387-396.
13. Maleki, Negar, Yasser Zeinali, and Seyed Taghi Akhavan Niaki. "A k-NN method for lung cancer prognosis with the use of a genetic algorithm for feature selection." *Expert Systems with Applications* 164 (2021): 113981.
14. Lavanya, M., P. Muthu Kannan, and M. Arivalagan. "Lung cancer diagnosis and staging using firefly algorithm fuzzy C-means segmentation and support vector machine classification of lung nodules." *International Journal of Biomedical Engineering and Technology* 37, no. 2 (2021): 185-200.
15. Bharati, Subrato, Prajoy Podder, and Pinto Kumar Paul. "Lung cancer recognition and prediction according to random forest ensemble and RUSBoost algorithm using LIDC data." *International Journal of Hybrid Intelligent Systems* 15, no. 2 (2019): 91-100.
16. Dev, Chethan, Kripa Kumar, Arjun Palathil, T. Anjali, and Vinitha Panicker. "Machine learning based approach for detection of lung cancer in dicom ct image." In *Ambient Communications and Computer Systems: RACCCS-2018*, pp. 161-173. Springer Singapore, 2019.
17. Radhika, P. R., Rakhi AS Nair, and G. Veena. "A comparative study of lung cancer detection using machine learning algorithms." In *2019 IEEE international conference on electrical, computer and communication technologies (ICECCT)*, pp. 1-4. IEEE, 2019.
18. Shakeel, P. Mohamed, Amr Tolba, Zafer Al-Makhadmeh, and Mustafa Musa Jaber. "Automatic detection of lung cancer from biomedical data set using discrete AdaBoost optimized ensemble learning generalized neural networks." *Neural Computing and Applications* 32 (2020): 777-790.
19. ALzubi, Jafar A., Balasubramaniyan Bharathikannan, Sudeep Tanwar, Ramachandran Manikandan, Ashish Khanna, and Chandrasekar Thaventhiran. "Boosted neural network ensemble classification for lung cancer disease diagnosis." *Applied Soft Computing* 80 (2019): 579-591.
20. Dodia, Shubham, B. Annappa, and Padukudru A. Mahesh. "Recent advancements in deep learning based lung cancer detection: A systematic review." *Engineering Applications of Artificial Intelligence* 116 (2022): 105490.
21. Pradhan, Kanchan, Priyanka Chawla, and Sanyog Rawat. "A deep learning-based approach for detection of lung cancer using self-adaptive sea lion optimization algorithm (SA-SLnO)." *Journal of Ambient Intelligence and Humanized Computing* 14, no. 9 (2023): 12933-12947.
22. Masood, Anum, Bin Sheng, Po Yang, Ping Li, Huating Li, Jinman Kim, and David Dagan Feng. "Automated decision support system for lung cancer detection and classification via enhanced RFCN with multilayer fusion RPN." *IEEE Transactions on Industrial Informatics* 16, no. 12 (2020): 7791-7801.
23. Huang, Nan, Liang Xiao, Qichao Liu, and Jocelyn Chanussot. "S 2 DMSC: A Self-supervised Deep Multi-level Subspace Clustering Approach for Large Hyperspectral Images." *IEEE Transactions on Geoscience and Remote Sensing* (2023).
24. Lanjewar, Madhusudan G., Kamini G. Panchbhai, and Panem Charanarur. "Lung cancer detection from CT scans using modified DenseNet with feature selection methods and ML classifiers." *Expert Systems with Applications* 224 (2023): 119961.
25. Pawar, A. B., M. A. Jawale, P. William, G. S. Chhabra, Dhananjay S. Rakshe, Sachin K. Korde, and Nikhil Marriwala. "Implementation of blockchain technology using extended CNN for lung cancer prediction." *Measurement: Sensors* 24 (2022): 100530.

26. Shakeel, P. Mohamed, M. A. Burhanuddin, and Mohammad Ishak Desa. "Automatic lung cancer detection from CT image using improved deep neural network and ensemble classifier." *Neural Computing and Applications* (2022): 1-14.
27. Gu, Chang, Chenyang Dai, Xin Shi, Zhiqiang Wu, and Chang Chen. "A cloud-based deep learning model in heterogeneous data integration system for lung cancer detection in medical industry 4.0." *Journal of Industrial Information Integration* 30 (2022): 100386.
28. Kasinathan, Gopi, and Selvakumar Jayakumar. "Cloud-based lung tumor detection and stage classification using deep learning techniques." *BioMed Research International* 2022 (2022).
29. Faruqui, Nuruzzaman, Mohammad Abu Yousuf, Md Whaiduzzaman, A. K. M. Azad, Alistair Barros, and Mohammad Ali Moni. "LungNet: A hybrid deep-CNN model for lung cancer diagnosis using CT and wearable sensor-based medical IoT data." *Computers in Biology and Medicine* 139 (2021): 104961.
30. Mishra, Sushruta, Hiren Kumar Thakkar, Pradeep Kumar Mallick, Prayag Tiwari, and Atif Alamri. "A sustainable IoHT based computationally intelligent healthcare monitoring system for lung cancer risk detection." *Sustainable Cities and Society* 72 (2021): 103079.
31. Bhujade, Vaishali G., Vijay Sambhe, and Biplab Banerjee. "Digital image noise removal towards soybean and cotton plant disease using image processing filters." *Expert Systems with Applications* 246 (2024): 123031.
32. Cao, Hu, Yueyue Wang, Joy Chen, Dongsheng Jiang, Xiaopeng Zhang, Qi Tian, and Manning Wang. "Swin-unet: Unet-like pure transformer for medical image segmentation." In *European conference on computer vision*, pp. 205-218. Cham: Springer Nature Switzerland, 2022.
33. Le, Dac-Nhuong, Velmurugan Subbiah Parvathy, Deepak Gupta, Ashish Khanna, Joel JPC Rodrigues, and K. Shankar. "IoT enabled depthwise separable convolution neural network with deep support vector machine for COVID-19 diagnosis and classification." *International journal of machine learning and cybernetics* (2021): 1-14.
34. Nazzal, Wasfieh, Karl Thurnhofer-Hemsi, and Ezequiel López-Rubio. "Improving Medical Image Segmentation Using Test-Time Augmentation with MedSAM." *Mathematics* 12, no. 24 (2024): 4003.
35. Thamilarasi V., Roselin. R., U-Net: Convolution Neural Network for Lung Image Segmentation and Classification in Chest X-Ray images, INFOCOMP, Vol. 20, No. 1, pp.101-108 (2021)